CANADIAN JOURNAL OF EXPLORATION GEOPHYSICS
VOL. 24, NO. 1 (JUNE 1988), P 66-71

A MODIFIED CURRENT-FILAMENT MODEL FOR USE IN THE INTERPRETATION OF FREQUENCY-DOMAIN ELECTROMAGNETIC DATA

K. DUCKWORTH[1]

ABSTRACT

A modified form of the current-filament (or single-turn current-loop) model used in the simulation of the electromagnetic response of thin, tabular, steeply dipping conductors is presented. The modification overcomes the inherent inability of the model to simulate the different spatial distributions of the real and imaginary components of the secondary field around a conductor at high frequencies. Theoretical and physical-model results are presented which demonstrate the benefits of the modification.

The modified model is also shown to provide the opportunity to reduce an observed Slingram profile to the single function which describes the geometric coupling between the target conductor and the transmitter and receiver coils. This form of output is shown to be free of the influence of the separation between the coils. In this form the data provided by a Slingram system can provide a direct measure of the relative magnitudes of the real and imaginary components of the induced current in a conductor. It also permits depth estimates to be obtained from the geometry of the reduced profiles.

The use of the closed-filament model for the simulation of the behaviour of conductors located in conductive host rocks is discussed and found to be inappropriate. An alternative approach employing combinations of individual line filaments, which works well in such circumstances, is discussed.

INTRODUCTION

The current-filament or single-turn coil model for a thin planar conductive ore body has proven to be a very useful simple tool for understanding the general behaviour of electromagnetic prospecting devices (Grant and West, 1965; Ward, 1970; Morrison et al., 1976; McCracken et al., 1986). In transient electromagnetic (TEM) surveys this model has recently been used as a direct interpretation tool, generating data which closely match observed decays of TEM fields at late time and providing numerical estimates of the location and geometry of conductors (Nabighian, 1978; Barnett, 1984; Becker et al., 1984; McNeill et al., 1984). However, the filament model has seen little use as a direct interpretation tool for frequency-domain electromagnetic (FEM) data. The following discussion demonstrates that the single-filament concept embodies limitations which prevent its use in the simulation of high-frequency FEM responses. A modification of the concept is described which overcomes these limitations while retaining the conceptual simplicity which is the reason for the use of the filament model. This approach does not attempt to provide a complete analytical solution for the response of a conductive tabular conductor, which is available in the work of Weidelt (1983).

THEORY

The frequency-domain behaviour of the filament model was treated by Grant and West (1965) who derived the following expression for the response of a small coil receiver over a tabular conductor simulated by a conductive closed-loop single-turn filament:

$$E_S/E_P = -\{(k_{01}k_{12})/k_{02}\}\{\alpha^2 + i\alpha)/(1 + \alpha^2)\} \quad (1)$$

where E_P and E_S are the primary and secondary signals detected by the receiver. The geometric constants k_{01}, k_{12} and k_{02} define the coupling between pairs of: the transmitter, the target and the receiver. The subscript 0 denotes the transmitter, 1 denotes the target and 2 denotes the receiver. The response parameter α is defined as $\alpha = \omega L/R$, where ω is angular frequency, L is the self-inductance of the target and R is its resistance.

Although this expression was originally developed for a dipole transmitter, it contains no term which specifies the form of the transmitter. Therefore, the expression applies equally well to devices using dipolar or large fixed-loop transmitters.

The three geometric constants in the coupling coefficient $\{(k_{01}k_{12})/k_{02}\}$ control the magnitude and geometry of the response. The complex response function $\{(\alpha^2 + i\alpha)/(1 + \alpha^2)\}$ contains no geometric terms; it only controls the relative magnitudes of the real and imaginary components of the response.

Manuscript received by the Editor August 18, 1987; revised manuscript received January 21, 1988.
[1]Department of Geology and Geophysics, The University of Calgary, Calgary, Alberta T2N 1N4.

Expression (1) implies that the ratio of the real component to the imaginary component of the response of a horizontal coplanar-coil moving-source (Slingram) device to a conductor simulated by a closed current filament will be independent of the separation between the transmitter and receiver. This contrasts with the well known behaviour of the real-to-imaginary ratio of the response of an actual tabular conductor detected by a Slingram device, which, for high frequencies, displays a strong dependence on the spacing of the transmitter and receiver. Hence, the single-turn coil or filament is inherently incapable of simulating this important feature of the response of a tabular conductor.

In view of this inherent limitation of the model for FEM modelling, it appears that similar problems must exist in its use in TEM modelling. That this is not well known can be seen in the remarks of Barnett (1984) where he asserts that it is intuitively obvious that a thin conductor can be represented by a single equivalent current filament at any instant in time. No verification of this assertion was provided.

Physical Model Results

Confirmation of this inherent limitation is provided by the comparison of the free-space analogue-model results for a Slingram device shown in Figure 1. The profiles in Figure 1a were obtained over a vertical, thin, rectangular, conductive sheet, while the profiles shown in Figure 1b were obtained (using the same frequency) over a rectangular wire frame (i.e., filament) with the same dimensions and depth as the sheet.

The vertical scales shown in these Figures display the signal amplitude as a percentage of the primary coupling for each case. However, each display has been magnified for display because of the wide disparity in the magnitudes of the anomalies. The vertical magnification factor is shown on each figure. The vertical percentage scales should be divided by the vertical magnification factor to give the true vertical scale of each profile.

The profiles in Figure 1b over the wire filament confirm that the real-to-imaginary ratio is independent of the spacing between the transmitter and receiver. The corre-

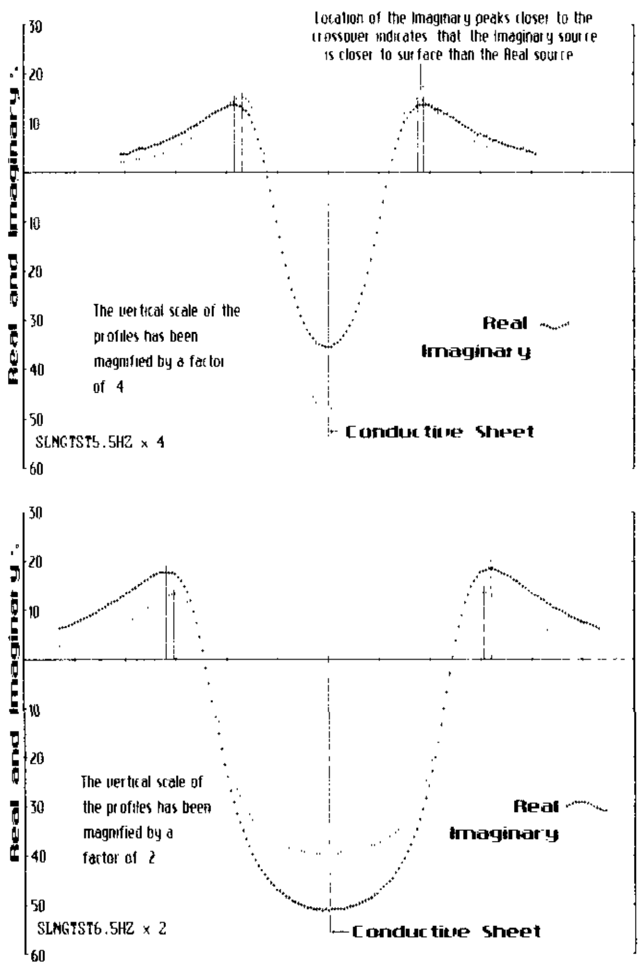

Fig. 1. (a) Slingram response profiles obtained over a vertical thin sheet conductor by means of analogue modelling using two Tx-Rx separations. Note the strong dependence of real-to-imaginary ratio on separation and the lack of coincidence between the locations of the real and imaginary peaks.

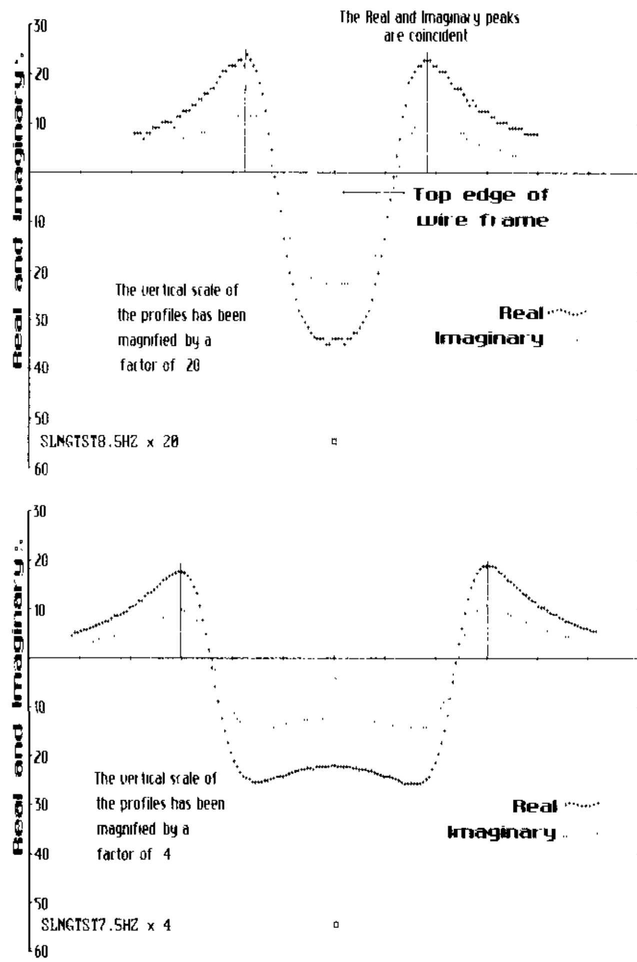

Fig. 1. (b) Analogue-model Slingram response profiles obtained over a wire frame with dimensions identical to the dimensions of the sheet conductor used to provide the profiles in Figure 1a. Note that the real-to-imaginary ratio does not change with separation and that the real and imaginary peaks are coincident.

sponding profiles in Figure 1a over the sheet target show the expected strong increase of the real-to-imaginary ratio as the separation is doubled. This effect is so pronounced that the relationship between the real and imaginary components inverts with the increase of separation. This allows the real to dominate for the large separation while the imaginary dominates for the small separation.

These profiles also show that for large transmitter-to-receiver separations, the geometry of the profiles obtained over the wire frame is poorly related to the geometry of the profiles over the sheet conductor. It is also notable that the amplitude of the filament response is very weak compared to that of the sheet.

This disparity in the geometry of the filament and sheet conductor profiles is caused by the fact that the sheet conductor tends to behave as a dipole source when a dipole transmitter is used. This was shown by Koefoed and Kegge (1968) and by Weidelt (1983). The length of the wire frame perpendicular to the traverse was approximately ten times the largest coil separation. Thus the system saw the top edge of the wire frame as a single line current, while the other edge and the ends were too distant to have any influence. At the large separation, each coil began to respond separately to this line current. Only at the small separation did the anomalies merge to produce the prominent central negative response which is a reasonable simulation of the response of a sheet conductor.

The cause of the dependence on coil separation shown by the real-to-imaginary ratio of the response of an actual sheet conductor must lie in the relative spatial geometry of the real and imaginary components of the secondary magnetic field around the conductor. This can be seen because the change of spacing between the transmitter and receiver can not alter the coupling between the transmitter and the conductor. Therefore, the coil separation can have no influence on the distribution of current within a conductor.

If the spatial distributions of these two components of the field are identical — as they must be if the target is a wire frame which forces both components of the secondary current to have identical geometry — then, at all points in space, the ratio of the magnitudes of the fields due to the two components will be constant. If the spatial distributions of these two field components are different, then the ratio can change with position and thereby also with separation. Clearly, the spatial distribution of the two components of the field around the conductor can only be different if each of the real and imaginary components of the current within the conductor has its own separate and different geometry.

The increase of the real-to-imaginary ratio as separation of the transmitter and receiver of a Slingram device is increased can only occur if the imaginary component of the secondary field around a conductor has a higher rate of geometric attenuation with distance from the conductor than has the real component of that field.

In the case of a Slingram device, the receiver detects the vertical component of the secondary field. This requires that the sources of the imaginary component of the field have a geometry which will provide this necessary higher rate of geometric attenuation of the vertical component. The simplest geometric difference between the sources of the two components of the field which will provide this effect is a difference in relative depth below surface. The shallower source will provide a vertical field component which attenuates more rapidly along the surface above the source than does the vertical component of the field due to a deeper source. For steeply dipping tabular conductors, this requires that the imaginary component of the induced current be concentrated closer to the top edge of the conductor than the real component. The physical-model profiles over a sheet shown in Figure 1a do, in fact, indicate a shallower depth of the imaginary source, because the positive shoulders on the imaginary-component profiles are closer to the crossover than are the corresponding shoulders on the real profiles. This behaviour was also shown by the theoretical profiles for good conductors provided by Weidelt (1983, Figure 7), and by the analogue-modelling results provided by Ketola and Puranen (1967, Figure 12), and by Nair et al. (1968, Figure 8).

Confirmation that at high frequency the imaginary component of the induced current concentrates closer to the edge of a sheet of conductor than does the real component is available in the theoretical work of Hanneson (1981, Figures 7 to 21), of Lajoie and West (1976, Figure 5), and of Lamontagne and West (1971).

At low frequencies or low conductivities, this same theoretical work shows that the geometries of the two components of the current induced to flow within a conductive body become almost identical. In such circumstances, the real and imaginary components of the secondary field around the conductor must have almost identical geometries. Thus, the ratio of their magnitudes will be approximately constant throughout space and thereby independent of the separation of the transmitter and receiver. This similarity of the geometries of the two components of the induced current would also cause the shoulders on the profiles of the real and imaginary components to be equally displaced from their respective crossovers and this is seen in the model results for moderate-to-poor conductors published by Ketola and Puranen (1967, Figures 27 and 32).

Thus the single-filament model can only simulate the behaviour of tabular conductors when the spatial distributions of the real and imaginary fields around such conductors are identical. However, even then, of course, it can not be an exact simulation.

In TEM work, a step-function change of the primary magnetic field is unable to diffuse instantly into a good conductor, so that for a short period after the change (a few microseconds) the induced effects are confined to the surface of the conductor, just as they are for high-frequency FEM fields (Oristaglio and Hohmann, 1984). At late time (after a few milliseconds), the change of field diffuses throughout the conductor, so that the induced current distribution becomes comparable to that which would be seen at low FEM frequencies where the induced currents flow throughout the whole volume of a conductor rather than being confined to its surface. Therefore, it is the late-time decay effects which correspond to the low-frequency or low-conductivity conditions which the single-filament model can simulate. However, the model must be just as inherently incapable of modelling the early-time TEM decays as it is of modelling the corresponding high frequencies in FEM. This explains the lack of success of the single-filament model in simulating early-time TEM responses and explains its notable success in late-time TEM work (Barnett, 1984; McNeill et al., 1984).

Modification of the Filament Model

The filament model can be modified so that it produces an acceptable (but never exact) simulation of the high-frequency (or high-conductance) behaviour of a sheet conductor. This requires that expression (1) be separated into its real and imaginary components and that each component be controlled by its own individual coupling coefficient. This follows from the fact that if — as is well established — the real and imaginary components of the current within the conductor have separate and different geometries, then each must be simulated by a separate and different filament, each of which requires its own coupling coefficient as follows:

$$E_S/E_P = -[\{(k_{R01}k_{R12})/k_{02}\}\{\alpha^2/(1+\alpha^2)\} + \{(k_{I01}k_{I12})/k_{02}\}\{i\alpha/(1+\alpha^2)\}] \quad (2)$$

It must be stressed that the filament model is only an empirical device which generates responses which resemble those of an actual conductor. This separation of the components is neither more nor less appropriate than the use of the original single-filament model for such simulations.

In the case of a horizontal coplanar-coil (Slingram-type) device, the geometric coupling function linking the transmitter to the target (k_{01}) and the function linking the target to the receiver (k_{12}) are exactly the same function. The principle of reciprocity requires that the form of this function be that of the vertical component of the field due to a current flowing in the conductive target. For a vertically dipping tabular conductor located in the field of a dipolar transmitter, Koefoed and Kegge (1968) and Weidelt (1983) found that the induced currents flow in localized loops which behave approximately as horizontal dipoles. Thus, a filament model which behaves as a horizontal dipole will be a good representation of the actual current in such a tabular conductor. For a horizontal magnetic dipole, the vertical component of its magnetic field, and therefore the coupling function, will have the functional form:

$$k_{01} = k_{12} = C(dx)/(x^2 + d^2)^{2.5} \quad (3)$$

where C is an arbitrary constant, d is the depth of the dipole and x is the distance along the traverse with the origin located on the surface directly above the dipole.

If C and d are allowed to adopt different values for the real and imaginary currents flowing in a conductor, then expression (3) can generate separate real and imaginary geometric coupling functions, as shown in Figure 2. In this case, the depth of the real source was made greater than that of the imaginary source and the value of C was made larger so that the real source would simulate a real current of greater magnitude than the imaginary current. Thus:

$$k_{R01} = k_{R12} = C_R(d_R x)/(x^2+d_R^2)^{2.5} \quad (4)$$

and

$$k_{I01} = k_{I12} = C_I(d_I x)/(x^2+ d_I^2)^{2.5} \quad (5)$$

where $C_R>C_I$ and $d_R>d_I$.

In the case shown in Figure 2 the following relationships were used:

$$C_R = 1.46\ C_I; \quad d_R = 1.2\ d_I.$$

The factors (1.46 and 1.2) in these expressions were arrived at by iterative adjustment of the theoretical profiles until a good match with the observed profiles of Figure 1a was obtained. They demonstrate that the magnitude of the real source was larger than that of the imaginary source — as is to be expected in a good conductor — while also confirming the shallower depth of the imaginary source.

The Slingram response profiles shown in Figure 2 were generated by taking the products of pairs of data points on the geometric coupling functions [i.e. $k_{R01}(x)k_{R12}(x + S)$

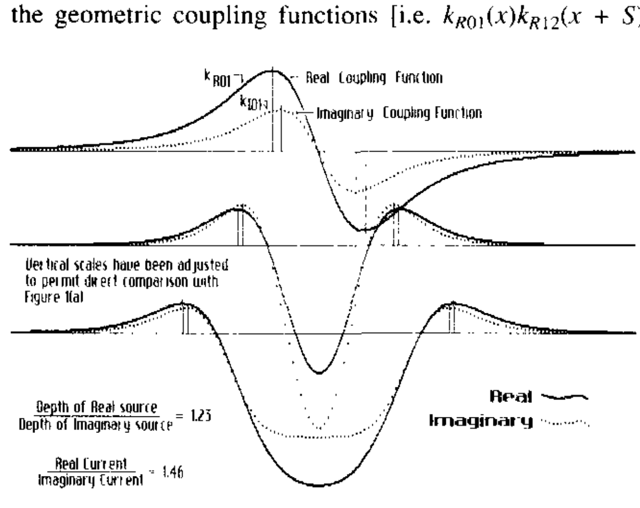

Fig. 2. These profiles were computed for a dipole target using the modified filament theory which allows the real-to-imaginary ratio to vary with spacing. Note the real and imaginary profiles display the same behaviour as the model profiles for the sheet conductor shown in Figure 1a both in terms of the lack of coincidence between the real and imaginary peaks and the strong attenuation of the imaginary response with increased spacing.

and $k_{I01}(x)k_{I12}(x + S)$ where S is the simulated separation between the coils]. Two separations were selected, differing by a factor of 2 as can be seen by the distance between the crossover points on the simulated Slingram profiles. It is necessary to emphasize that the two sets of Slingram-type profiles shown in Figure 2 have a common origin in the coupling functions shown at the top of that Figure. The only change in the operation performed on the coupling functions to generate the Slingram profiles was to change the simulated separation between the coils.

Comparison of these generated profiles with the corresponding physical-model profiles in Figure 1a for the sheet conductor shows a very good match. The doubling of the separation in both the physical-model and the theoretical profiles produced a relative enhancement of the real component which resulted in that component becoming dominant at the large separation. The theoretical curves also show the disparity of locations between the real and imaginary positive shoulders, with the imaginary shoulders being closer to the crossovers due to the shallower depth of their source. This disparity comes from the depth disparity which is built into the two coupling functions and which appears in those functions as a lack of coincidence of the maxima.

While the match achieved with Figure 1a is good in terms of the relative behaviour of the real and imaginary profiles, it is poor in terms of the relative magnitudes of the positive shoulders with respect to the central negative on each profile. This possibly results from the fact that in the actual conductor the locations of the real and imaginary sources within the conductor will change with the distance of the transmitter from the conductor, while in the filament simulation the two sources are fixed at their separate depths regardless of the location of the transmitter. It might be possible to improve the match by allowing the depth of each source to be a function of the transmitter distance.

It should be noted that the theoretical profiles of Figure 2 are presented with the same vertical amplification as used in Figure 1a. For a particular spacing, the real and imaginary profiles have the same scale so that their relative behaviour is not affected; nor is their geometry.

While the sources of the real and imaginary fields in this example were chosen to be dipoles, this approach could use separate rectangular filament sources for the two components of the field or any type of source that is best suited to a particular type of ore target.

Potential Benefits of Inversion to the Coupling Function

Figure 2 illustrates a possible additional benefit of this matching of recorded Slingram profiles with synthetic profiles. This benefit arises in the matching process, where the observed profiles are effectively inverted to coupling functions which are free of the strong influence that the separation of the transmitter and receiver has on the recorded Slingram profiles. Such an inversion applied to profiles recorded over different prospects would allow them to be compared directly in the coupling-function form, even if the profiles were recorded with widely different coil separations.

If the inversion is achieved by iterative forward modelling, the process automatically provides a measure of the conductor quality in the ratio of the constants C_R and C_I. It also produces depth values d_R and d_I. However, a more intriguing possibility is that observed profiles could be inverted directly to the coupling-function form in a single-step process without reference to the filament model or any other model. Full development of this concept is beyond the scope of the present discussion. However, it can be seen that direct inversion will be possible in cases where two sets of profiles over the same conductor with different spacings are available. In such a case, the inversion would be no more than a matter of solving simultaneous equations. Direct inversion of this kind would produce functions which would have a real-to-imaginary ratio which would be independent of instrumental conditions. This ratio would directly reflect the ratio of the magnitudes of the real and imaginary currents induced into the conductor. In addition, the depth of a conductor could be derived directly from the lateral separation between the maximum and minimum on the coupling function (as can be seen in Figure 2) rather than from amplitude data taken from the Slingram profiles plotted on anomaly-index diagrams of the type provided by Nair et al. (1968). The lateral geometry of the coupling funciton would not be affected by the calibration of the instrument, while use of the anomaly-index type of diagram requires careful attention to this calibration.

Reducing Slingram profiles to the coupling functions would also have the benefit of allowing moving-source data to be compared directly with fixed-source data because the coupling functions of line 1 in Figure 2 are what would be seen directly by a fixed-source device. (That is, provided a correction were applied for the effect of the variation of the k_{02} coupling of the transmitter to the receiver, only k_{R12} and k_{I12} in expression (2) would vary in such a case.)

Application of the Filament Model in Conductive Environments

For a conductor located in a conductive host environment, the currents flowing in the conductor will be a combination of directly induced current and current gathered from the conductive host environment. The current gathered from the host will have the same direction throughout the conductor, as shown by Lajoie and West (1976, Figure 6). This means that the directly induced closed-vortex current (Lajoie and West, 1976, Figure 5) must oppose the gathered current in one edge of the conductor while flowing with the gathered current in the other edge. Thus, the net currents flowing along the edges of a conductor located in a conductive host rock will not be equal, whereas they would be in any closed-loop filament model.

If, in such circumstances, the closed-filament model is abandoned in favour of individual line filaments, the currents in the various edges of the conductor can be treated independently so that the magnitude and phase of the current in each line filament can more closely simulate the actual net currents in the conductor. If desired, the rectangular type of filament can be constructed from four short line elements. Alternatively, individual line elements can be used separately without concern for creating closed loops, because this is no more than an empirical device which does not have to resemble the physical system it is simulating. Nor does it necessarily have to obey the physical laws which govern the system being simulated.

The use of a model based on individual line filaments allows any number of line filaments to be used where they are needed to simulate separate edge effects that occur in wide conductors. This approach is very effective and economical in the interpretation of data acquired with fixed rectangular-loop-type transmitters (Duckworth, 1972).

Complete solutions for the electromagnetic response of localized conductors are available (Hohmann, 1975; Lajoie and West, 1976; Weidelt, 1983; Hanneson and West, 1984) but they are computationally demanding. The use of two-dimensional modelling can provide a useful reduction in computing costs, but, in electromagnetic modelling, the two-dimensional approximation is inherently incapable of dealing with the effect of current gathering in conductive environments (Nabighian, 1984). In these circumstances the full 3-dimensional approach must be used. However — as an alternative to the high-cost 3-dimensional methods — the line-filament concept can be applied empirically to data acquired in conductive environments with any desktop microcomputer (Duckworth, 1972) and can provide useful interpretation of such data.

CONCLUSIONS

Modification of the filament model to allow separate simulations of the real and imaginary components of the current induced into a conductor provides a useful extension of the capabilities of the model while retaining the simplicity which is the most valuable feature of the concept.

This modified form of the model appears to offer the interpreter a means to extend the range of application of the model from its present success in late-time TEM modelling to the treatment of high-frequency FEM effects for both moving-source and fixed-source devices.

As the concept is only an empirical tool, which need not obey the physical laws of the system which it is used to simulate, there is no intrinsic reason why the filament must form a closed loop. By adopting a line-filament concept it becomes possible — by using combinations of such line filaments — to treat a wider range of cases, among which the conductive-host case is of particular importance.

REFERENCES

Barnett, C.T., 1984, Simple inversion of time-domain electromagnetic data: Geophysics **49**, 925-933.

Becker, A., DeCarle, R. and Lazenby, P.G., 1984, Simplified prediction of transient electromagnetic response: Geophysics **49**, 913-917.

Duckworth, K., 1972, Turam interpretation by curve matching using a line current approximation: Geophys. Prosp. **20**, 514-528.

Grant, F.S. and West, G.F., 1965, Intepretation theory in applied geophysics: McGraw-Hill Book Co.

Hanneson, J.E., 1981, The horizontal loop EM response of a thin vertical conductor in a conducting half space: Ph.D. thesis, Univ. of Manitoba.

_____ and West, G.F., 1984, The horizontal loop electromagnetic response of a thin plate in a conductive earth: Part II — Computational results and examples: Geophysics **49**, 421-432.

Hohmann, G.W., 1975, Three-dimensional induced polarization and electromagnetic modelling: Geophysics **40**, 309-324.

Ketola, M. and Puranen, M., 1967, Type curves for the interpretation of Slingram horizontal loop anomalies over tabular bodies: Geol. Surv. Finland, Rep. of Investigations No. 1.

Koefoed, O. and Kegge, G., 1968, The electrical current pattern induced by an oscillating magnetic dipole in a semi-infinite thin plate of infinitesimal resistivity: Geophys. Prosp. **16**, 144-158.

Lajoie, J.J. and West, G.F., 1976, The electromagnetic response of a conductive inhomogeneity in a layered earth: Geophysics **41**, 1133-1156.

Lamontagne, Y. and West, G.F., 1971, EM response of a rectangular thin plate: Geophysics **36**, 1204-1222.

McCracken, K.G., Oristaglio, M.L. and Hohmann, G.W., 1986, A comparison of electromagnetic exploration systems: Geophysics **51**, 810-832.

McNeill, J.D., Edwards, R.N. and Levy, G.M., 1984, Approximate calculation of the transient electromagnetic response from buried conductors in a conductive half-space: Geophysics **49**, 918-924.

Morrison, H.F., Dolan, W.M. and Dey, A., 1976, Earth conductivity determinations using a single superconducting coil: Geophysics **41**, 1184-1206.

Nabighian, M.N., 1978, Size determination from EMP data: In-house Rep., Newmont Exploration Ltd.

______, 1984, Foreword and introduction to special issue of Geophysics on time-domain electromagnetic methods of exploration: Geophysics **49**, 849-853.

Nair, M.R., Biswas, S.K. and Mazumdar, K., 1968, Experimental studies on the electromagnetic response of tilted conducting half-planes to a horizontal-loop prospecting system: Geoexplor. **6**, 207-244.

Oristaglio, M.L. and Hohmann, G.W., 1984, Diffusion of electromagnetic fields into a two-dimensional earth: A finite-difference approach: Geophysics **49**, 870-894.

Ward, S.H., 1970, Airborne electromagnetic methods: Mining and groundwater geophysics/1967: Geol. Surv. Can., Econ. Rep. No. 26, 81-108.

Weidelt, P., 1983, The harmonic and transient electromagnetic response of a thin dipping dike: Geophysics **48**, 934-952.